

# Biomass Production of Microalgae *Scenedesmus* in a Raceway and Tubular Photobioreactor

José F. Reyes, Paulina J. Vielma, Wilson D. Esquivel and Johannes P. de Brujin

Faculty of Agricultural Engineering, Universidad de Concepción, Casilla 537, Chillán, Chile

**Abstract:** A comparison of culture biomass evolution for the microalgae *Scenedesmus spinosus* in a tubular pilot photobioreactor of 1.6 m<sup>3</sup> and a raceway pilot photobioreactor of 1.2 m<sup>3</sup> was carried out, using a nutritional Z-8 medium with the injection of carbon dioxide, and using an electronic system for monitoring and control of operational variables. For three weeks of testing, each culture was exposed to three pH levels of 6.5, 7.0 or 7.5, where random samples from both bioreactors were taken three times a week, to analyze pH, turbidity, transmittance at 640 nm and temperature. At the beginning and the end of culture, total solids were analyzed, and photographs were taken with a microscope to study the cell conditions of culture. This study revealed that the highest biomass production of *Scenedesmus spinosus* was obtained at pH 6.5 in the raceway photobioreactor, with a productivity of 371 g m<sup>-3</sup> day<sup>-1</sup>, 0.78 % total solids, a turbidity of 858 NTU and 5% transmittance at the end of the culture.

**Key words:** Microalgae, photobioreactor, biomass, raceway, tubular.

## 1. Introduction

The environmental pollution caused by the excess of human energy consumption and the foreseeable depletion of fossil fuels underline the need for new, environmentally sustainable, and cost-effective energy sources. One of the possible sources of renewable energy is biofuels. Microalgae can be used to produce biodiesel, bioethanol, methane or hydrogen [1-3]. Recent research works on microalgae have identified this new bio-material as a promising technology for bioenergy production, wastewater treatment, the development of high value added products and CO<sub>2</sub> capture [4-6]. It has also been proposed to use it as a substrate to generate energy through Microbial Fuel Cells [7]. Algae are non-vascular photosynthetic plants that contain chlorophyll and possess simple reproductive structures and limited mobility. Most of these are microscopic, which are called microalgae [8]. Unlike higher plants, they contain relatively small amounts of structural material and many of the cellular components are of recognized economic value. They contain a large number of essential pigments,

under the action of sunlight and simple inorganic substances such as carbon dioxide, nitrogenous and phosphorous compounds. Through the photosynthetic process, they are transformed into complex organic compounds such as carbohydrates, lipids, proteins, etc., which subsequently accumulate in cells, and in the tissues of simple and higher organisms [9, 10]. From the biomass generated it is possible to extract oil to make biodiesel through transesterification reactions [11]. There are also results of biodiesel production studies by direct transesterification of microalgae biomass, avoiding the oil extraction stage [12, 13]. The enhancement of the lipid content in microalgae strains without decreasing the growth rate is a prerequisite for improving the economic viability of microalgae-derived biofuel production. The implementation of an appropriate cultivation strategy can increase both lipid accumulation and biomass production [14]. Cumulative impact of salinity, carbon sources such as glycerol and glucose and photoperiod on the cultivation of the microalgae in mixotrophic growth in pure air supplied photobioreactors aiming at biomass output and lipid

**Corresponding author:** José F. Reyes, Ph.D., research fields: agricultural and electrical engineering, biofuels and automation.

content enhancement for increased biodiesel productivity, has been studied recently [11]. One of the species of green algae most used in the development of biodiesel is *Botryococcus braunii*. Regarding to these microalgae, Maxwell et al. and Brown et al. [15, 16] state that *Botryococcus braunii* is a unicellular microalga that in relation to its dry weight, directly produces a high percentage of hydrocarbons which it then excretes. Fierro-Reséndiz [17] evaluated the growth rate of three strains, among which is *Scenedesmus spinosus*. These were cultivated at 20 °C and 32 °C, obtaining the highest growth rates at a temperature of 32 °C. For the genus *Scenedesmus* sp., a lipid concentration of 15 to 35% was reported. New research usage of improved medium composition for enhanced biomass, lipid and starch content for the heterotrophic cultivation of *Scenedesmus* sp. has been reported, with maximum biomass yield of 5.02 g L<sup>-1</sup> [18]. Other study evaluated the combined effects of trace elements, salinity stress and different cultivation modes on lipid productivity of the freshwater *scenedesmus* strains. In that cultivation, applying culture medium supplemented with trace elements and salt stress, sustained a higher production of lipids [19]. Nowadays researchers are nominating microalgae for the efficient treatment of effluents as well as producing plenty of value-added products by the excessive nutrient's removal from the waste effluents. High phosphate and nitrogen elimination have been observed with high microalgae growth and biomass production of up to 5.27 g L<sup>-1</sup> [20].

One of the main issues in biomass microalgae production is related to the photobioreactor design and its configuration which determines the gas-liquid transfer and solar input efficiency. Some of these considerations and additional technical-economic comparison are addressed in one research [21] which analyzes the open and close photobioreactor microalgae production. The other important aspect is related to photobioreactor operation process conditions in order to get the maximum biomass productivity. Those parameters are related mainly to nutritional formulas, culture stirring

level and pH, in order to optimize biomass output which is analyzed in a publication [22]. In this research, comparative photobioreactor design under Z-8 nutritional conditions was studied using a *scenedesmus* sp. microalgae strain.

## 2. Experimental Setup

### 2.1 Pilot Photobioreactor Inoculum

A sample of 2.3 L of *Scenedesmus spinosus* provided by the Department of Biology of the University of Concepción, Chile, was used as inoculum. The turbidity of the initial culture was determined by means of a turbidimeter Hach Lange, 2100P, corresponding to 92.7 ± 25.9 NTU. The inoculation was started in two cylindrical air-lift type polycarbonate photobioreactors illustrated in Fig. 1. These reactors are made of polycarbonate, 0.3 m in diameter, 0.5 meters high and with a useful volume of 30 L. At the base of each reactor a 0.2 m diameter perforated circular plate was installed with 110 perforations of 1 mm diameter for the injection of air through the base, by means of a compressor AB100-24BM, BAUKER. The reactors were located inside a chamber illuminated by 18 fluorescent tubes each with a power of 18 W and an air conditioning system Galanz 12,000 BTU cold/heat. In this way, an ascending liquid circulation was generated in the center of the reactors, and descending in the peripheral circular ring, for an adequate stirring and solubility of the CO<sub>2</sub>. These two reactors were each inoculated with 1.15 L of inoculum, obtaining a total volume of 11.5 L using the Z-8 culture medium for each reactor. During cultivation, these were kept at a light intensity that fluctuated between 110 and 424 lux, under continuous illumination, a temperature of 25 °C and a pH between 6.5 and 7.0 for a period of 31 days after starting the process.

The culture generated in the phase just described, was used as inoculum in the next step that corresponded to the culture at a scale of 300 L and considered a first series of five 30 L photobioreactors (150 L) of the type shown in Fig. 1. These were maintained at a light

intensity that fluctuated between 110-424 lux, with a photoperiod of 10 hours of illumination. The second series of five similar photobioreactors (R6-R10) with another 150 L were maintained at a light intensity that fluctuated between 115-450 lux with the same photoperiod as the previous phase. The final culture generated as described by this protocol, was used as inoculum in both pilot bioreactors, using 480 liters of inoculum in the tubular bioreactor and 360 liters in the raceway bioreactor. In both cases, there was a control over the air flow and the percentage of CO<sub>2</sub> injected into the system by means of an automated control system.

## 2.2 Pilot Tubular Airlift Photobioreactor

A pilot air-lift reactor was used which is shown in Fig. 2B. The bioreactor used consisted of four vertical and four horizontal tubes with a height of 2.5 m each, a diameter of 0.31 m and a total volume of 1.4 m<sup>3</sup>. At the top, four sensors were installed to record, pH, temperature, irradiation and dissolved oxygen. This data acquisition kit had a 4-20 mA analog output, and 270 Ohm resistors to generate an output electrical potential between 0 to 5 V, which was digitized by a microcontroller [21]. The system also controlled CO<sub>2</sub> concentration through indirect pH measurement, according to the experimental calibration curve shown in Fig. 3.



Fig. 1 Laboratory airlift photobioreactors.

## 2.3 Pilot Raceway Photobioreactor

A pilot raceway shaped reactor was used whose image is shown in Fig. 2A, with dimensions of 40 cm high, 5 m long, 94 cm wide and a usable volume of 1.2 m<sup>3</sup>, constructed of fiberglass and covered with a transparent polycarbonate lid on top, and a paddle stirrer connected to a Gearmotor, 12 VDC, 50 RPM. The reactor had forty CO<sub>2</sub> injection points at its base and with sensors located on one superior corner, registering pH, temperature, radiation and dissolved oxygen. These devices had a standard 4-20 mA analog output, and 270 Ohm resistors to generate an output electrical potential between 0 to 5 V, which was digitized by a microcontroller [21]. The system also controlled CO<sub>2</sub> concentration through indirect pH measurement, according to the experimental calibration curve shown in Fig. 3.



Fig. 2 (A) Tubular airlift pilot photobioreactor, (B) Raceway pilot photobioreactor.

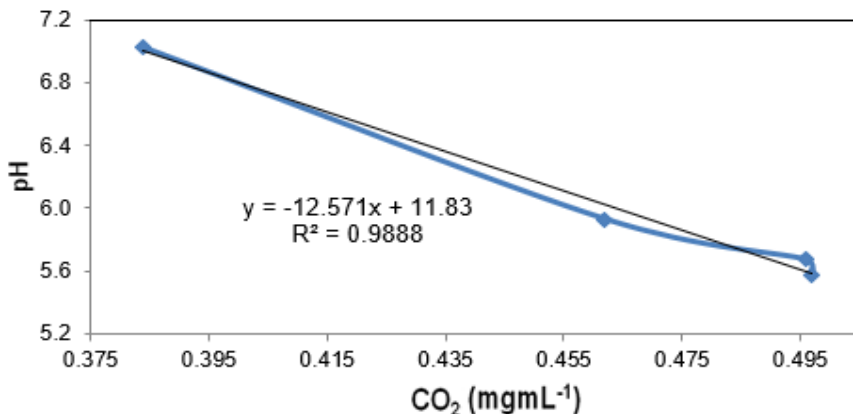


**Fig. 3** Relationship between pH and the concentration of dissolved CO<sub>2</sub> in the microalgae culture.

**Table 1** Z-8 culture medium.

Compound	Mass (g/24 L <sub>H2O</sub> )
NaNO <sub>3</sub>	1,120.8
K <sub>2</sub> HPO <sub>4</sub>	74.4
Na <sub>2</sub> CO <sub>3</sub>	50.4
Ca(NO <sub>3</sub> ) <sub>2</sub> 4H <sub>2</sub> O	141.6
MgSO <sub>4</sub> x 7H <sub>2</sub> O	60.0
Fe-EDTA	93.6
Trace elements stock solution	1,200 ML

#### 2.4 Culture Medium

For the culture implemented to produce the inoculum of the laboratory photobioreactors, and also in the tests carried out in the p3ilot-scale photobioreactors, the nutritional medium Z8 was used, whose chemical composition is detailed in Table 1 for a volume of 24 liters. The chemical components of each media were added to the pilot bioreactors proportionally to the volume of each reactor.

#### 2.5 Turbidity and Transmittance

The growth of the microalgae was determined using the 2100P turbidimeter, HACH, range 0 to 1,000 NTU (Nephelometric Turbidity Units). The percentage of transmittance of the microalgae suspension was measured using a Spectronic 20d spectrophotometer, Bausch & Long, at 640 nm. In both cases, the measurement was carried out with respect to a culture medium in absence of microalgae strain.

#### 2.6 Total Solids

To determine the total solids, 20 mL of the microalgae suspension in a Petri capsule was used, whose mass was determined on an Electronic Balance scale, FA2104N and then they were kept in a Gallenkamp oven, Hotbox oven at 103-105 °C, until the sample was dry. The capsules were then placed in a desiccator until room temperature was reached, and then their mass was determined. This operation was repeated until reaching constant mass, for 48 hours.

#### 2.7 Microscopy

A drop of the microalgae suspension was placed on a slide and taken to a Zeiss microscope, Axiostar with an AOC computer, OVER 450 and then the digitized image was saved (Canon Digital Solution Disk v26, Zoom Browse EX v5.5).

#### 2.8 Statistical Analysis

To evaluate differences in growth between the trials, ANOVA (analysis of variance), including the F test, to check if there are significant differences between the mean values of the tests and the LDS (Low Density Solids) test for multiple comparison between trials, determining which present significant difference, applied to the values of: turbidity, transmittance and total solids. The statistical program used in the analysis of the results was Statgraphics centurion XVI, with a confidence interval of 95%.

### 3. Results

Analyzing Fig. 4A, for the tubular bioreactor, a very moderate growth of microalgae could be seen until day 10, after this day there were a maximum turbidity value at pH 7.5 with 327 NTU. The tests at pH 6.5 and 7.0 reached their maximum value on day 18 with 322 NTU and 284 NTU, respectively. However, for the three trials, there was a phase of decline in growth after day 14. Fig. 4B for the raceway bioreactor indicates better results, where the growth of microalgae was exponential for the three tests until day 12, like the tubular reactor, continued by a stationary phase. At pH 6.5 the greatest turbidity difference of the three tests was achieved, from day 0 to 21 increasing from 158 NTU to 858 NTU, followed by the test at pH 7.0 that increased from 507 NTU to 947 NTU while the test at pH 7.5 registered a smaller difference in initial and final turbidity with 213 NTU and 533 NTU, respectively. Comparing both reactors, it is clear that the growth in the tubular bioreactor was slower, in contrast to the raceway bioreactor, where the growth of the culture was exponential, multiplying up to eight times the initial turbidity value for the three pH levels.

According to Fig. 5A it can be seen that for pH 6.5, in the tubular bioreactor the culture began with a transmittance of 55 % while on day 18 reached its minimum of 40 % and then 49 % on day 21. At pH 7.0 the evolution was similar to the previous test, starting with 45 % of transmittance until reaching 33 % on the day 21. For pH 7.5 the greatest difference was observed

between the initial and final transmittance, decreasing at 21 days by 41%. However, comparing the three transmittance profiles of the tubular bioreactor, starting at day 12, a small transmittance decrease for pH 6.5 and 7, and an increase for pH 7.5 are clearly observed, which could be interpreted as a stationary phase in growth. Fig. 5B, shows that for the pH 6.5 test in the raceway bioreactor, the most dilute culture was obtained starting with transmittance of 64%, reaching 5% at day 21; then the decrease in transmittance was proportional and rapid until day 10, subsequently the transmittance decreased negligibly, compared to the first 10 days. On the other hand, the pH 7.0 test showed a gradual decrease in transmittance until day 12. However, in the interval between the initial and final transmittance, a change from 20% and 3% respectively was observed. For the test at pH 7.5 on day 0, a transmittance of 46 % was measured, and after the first 5 days there was a decrease in transmittance, except for day 7. At the end of each test, the final transmittance levels in the tubular bioreactor as indicate Figure 5A, showed higher values with respect to the raceway bioreactor. The final transmittance in the raceway bioreactor was clearly lower and very similar for different pH levels as indicate Fig. 5B.

In Fig. 6, the temperature range along the culture period is shown, being 31.5 °C the maximum value for the tubular and 27.7 °C for the raceway bioreactor, which allowed reaching high final turbidity levels of 141 NTU and 858 NTU, respectively. The temperature during the growth of microalgae showed to be a

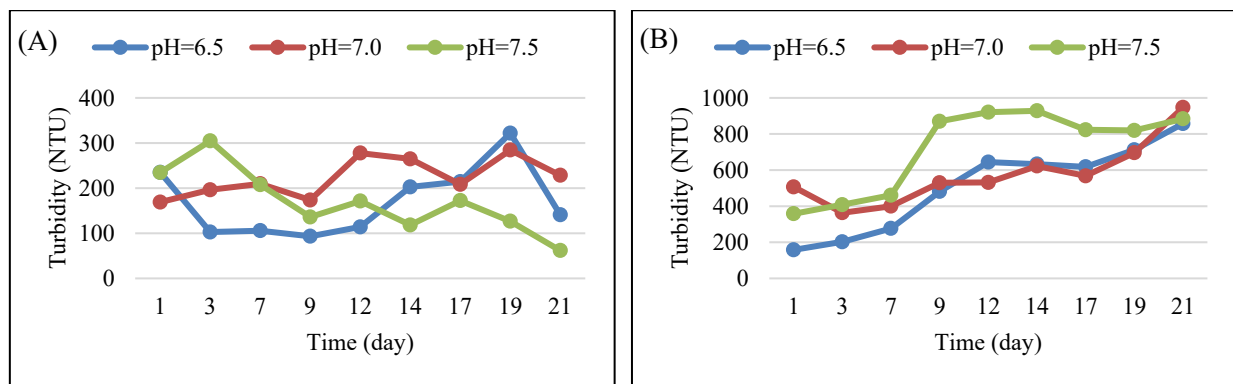


Fig. 4 Turbidity evolution of cultures: (A) Tubular photobioreactor, (B) Raceway photobioreactor.

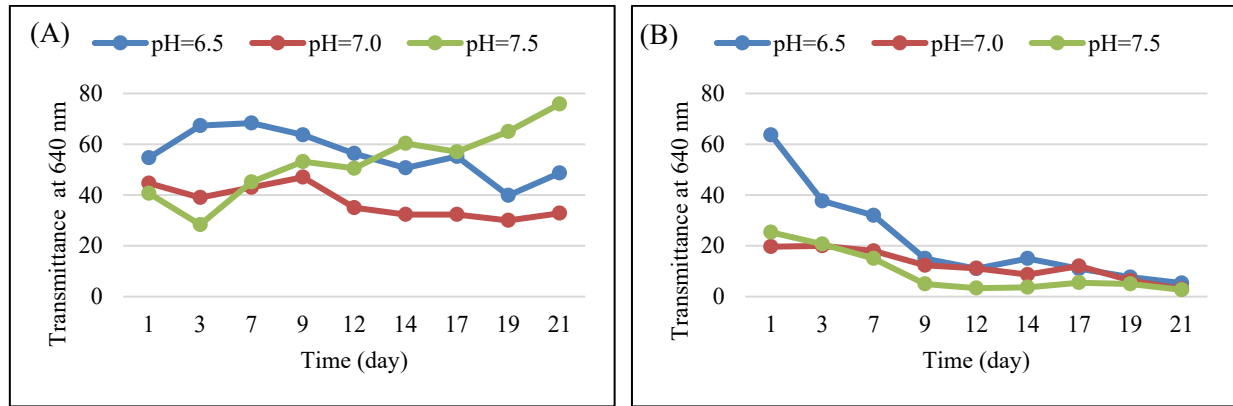


Fig. 5 Transmittance evolution of cultures: (A) Tubular photobioreactor, (B) Raceway photobioreactor.

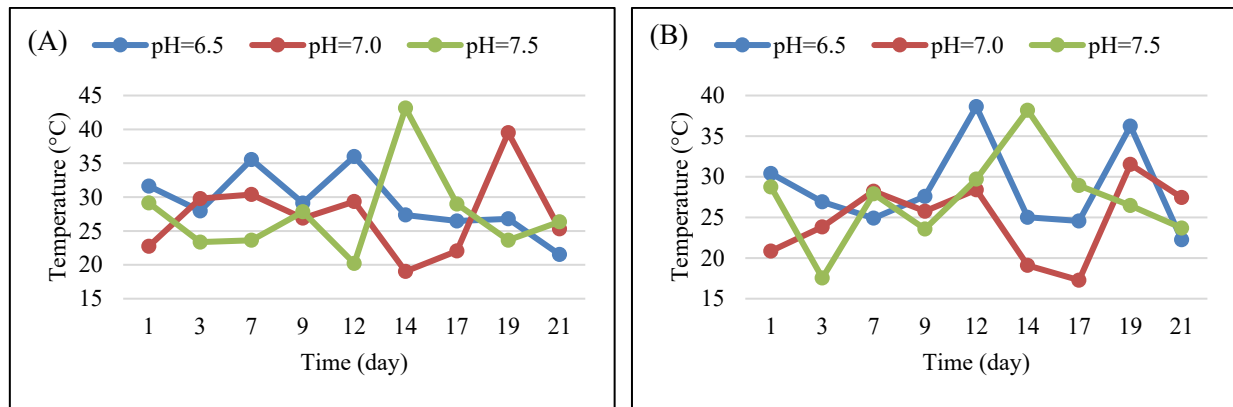


Fig. 6 Temperature evolution of cultures: (A) Tubular photobioreactor, (B) Raceway photobioreactor.

limiting factor, since it is related to the irradiation photosynthetic intensity. Under these conditions there is no doubt that if Figs. 4A and 6A for the tubular bioreactor are analyzed together, there is a dependent behavior, since turbidity increases if the temperature increases, as is the case on day 10 where for pH 6.5 the temperature reached a maximum of 36 °C and turbidity increased, as long as at pH 7.0 on day 18, with a maximum temperature of 39.5 °C and a maximum of turbidity of 284 NTU. The same occurs at pH 7.5 where the maximum temperature of 44 °C was obtained on day 10, with a maximum in turbidity of 327 NTU. Similar tendencies were observed for the raceway reactor in Figs. 4B and 6B, showing that at pH 6.5 on day 10 the maximum temperature of 38.6 °C was coincident with a turbidity increment until reaching 858 NTU. For pH 7.0 occurred some differences since the minimum temperatures were obtained between days 10 and 14, when the culture was in a linear growth stage.

In the test at pH 7.5 the culture lowest temperatures were recorded between days 12 and 21, when the culture began a phase of decline in turbidity. The maximum and minimum temperature in the tubular reactor were 44 °C and 19 °C respectively, while in the raceway bioreactor the maximum and minimum temperatures were 41 °C and 17 °C respectively. The maximum temperature values are consistent with the irradiation levels of Fig. 7, which implicated average values of 1,374.2, 1,376.2 and 1,418.7 w m<sup>-2</sup> at pH 6.5, 7.0 and 7.5 respectively, for the tubular bioreactor. The lower average values of 845.2, 922.9 and 912.9 w m<sup>-2</sup> found for the raceway bioreactor generate a lower maximum temperature as shown in Fig. 6. It is interesting to note that the maximum temperature in the raceway bioreactor was high enough, despite the fact that the irradiation levels were significantly lower as depicted in Fig. 7. This indicates that the tubular bioreactor was able to behave more efficiently from a

thermal point of view, probably due to its design characteristics. On the other hand, despite the lower intensity of irradiation received, the tubular bioreactor exhibited higher rates of biomass growth, as indicated in the Figs. 4 and 5.

Fig. 8 illustrates the pH variation profile measured over time in each of the tests. In the tubular bioreactor the pH levels were closer to each other and in general with pH values lower than the desired level as shown in Fig. 8A. For this bioreactor the highest control accuracy was achieved for pH 6.5, while for pH 7.0 and 7.5 levels, the values were generally slightly lower than the targeted value. With respect to the raceway bioreactor, Figure 8B indicates that the carbon dioxide injection control system allowed a greater differentiation between the three pH levels and that the pH values were closer to the desired setpoints.

The biomass productivity results under different pH conditions, shown in Table 2, clearly indicate the superiority of the raceway bioreactor at pH 6.5. Since at a lower pH the density of dissolved CO<sub>2</sub> increases in the culture, this may favor the kinetics of algal growth. The final concentration of solids in the culture, for both bioreactors and the consequent productivity of biomass obtained at pH 6.5, reflects this reality. These results are reinforced when reviewing Table 3, which shows that the raceway bioreactor generated higher productivity, although the average irradiation in the tubular bioreactor was notoriously higher. At the same time, it is observed that the average temperatures do not show significant differences between both bioreactors, indicating that the modified raceway bioreactor design presented better thermal efficiency during the tests.

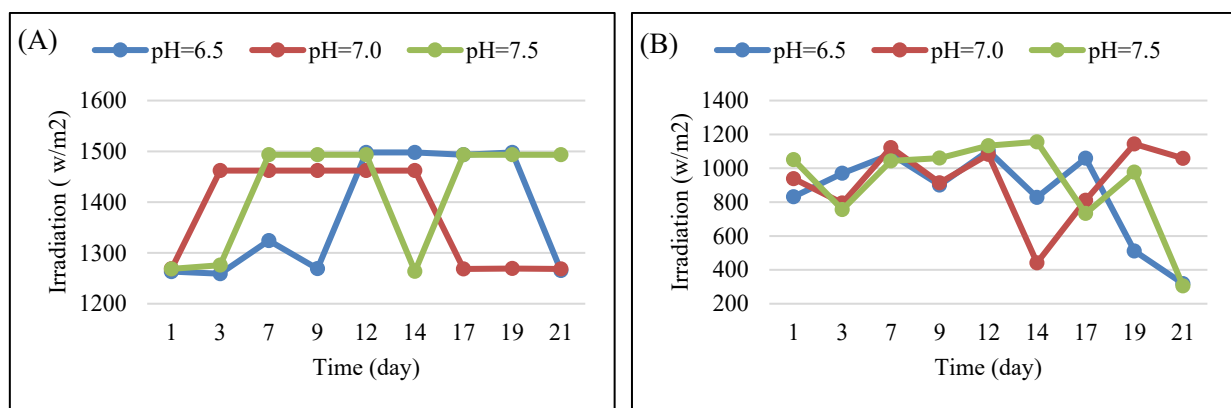


Fig. 7 Irradiation evolution of cultures: (A) Tubular photobioreactor, (B) Raceway photobioreactor.

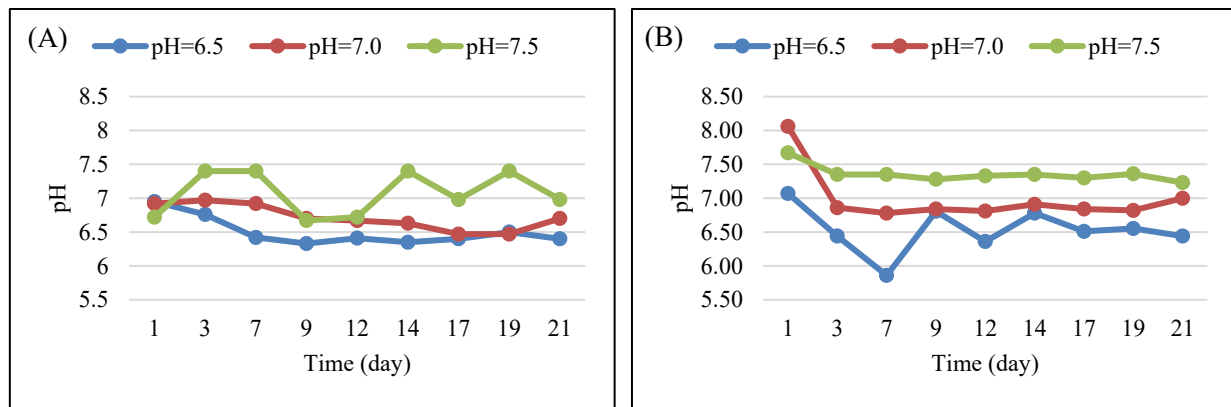


Fig. 8 Evolution of culture pH: (A) Tubular photobioreactor, (B) Raceway photobioreactor.

**Table 2** Culture productivity.

pH	Tubular photobioreactor		Raceway photobioreactor	
	Final solids (% w/w)	Productivity (g m <sup>-3</sup> d <sup>-1</sup> )	Final solids (% w/w)	Productivity (g m <sup>-3</sup> d <sup>-1</sup> )
6.5	0.7 ± 0.06 <sup>b*</sup>	333 ± 29	0.79 ± 0.01 <sup>c</sup>	371 ± 5
7.0	0.1 ± 0.00 <sup>a</sup>	48 ± 0.00	0.1 ± 0.00 <sup>b</sup>	48 ± 0.00
7.5	0.1 ± 0.00 <sup>a</sup>	48 ± 0.00	0.06 ± 0.00 <sup>a</sup>	33 ± 0.00

\* Same letters in the vertical direction indicate there is not significant difference according to the LSD test with 95% confidence.

**Table 3** Culture average variables.

pH	Tubular photobioreactor			Raceway photobioreactor	
	Irradiation (w m <sup>-2</sup> )	Temperature (°C)	pH	Irradiation (w m <sup>-2</sup> )	Temperature (°C)
6.5	1,374.2 <sup>a*</sup>	29.2 <sup>b</sup>	6.5	845.2 <sup>a</sup>	28.5 <sup>b</sup>
6.7	1,376.2 <sup>a</sup>	27.2 <sup>a</sup>	7.0	922.9 <sup>b</sup>	24.7 <sup>a</sup>
7.1	1,418.7 <sup>b</sup>	27.4 <sup>a</sup>	7.4	912.9 <sup>b</sup>	27.2 <sup>b</sup>

\* Same letters in the vertical direction indicate there is not significant difference according to the LSD test with 95% confidence.

In Fig. 9, at the end of the culture, at pH 6.5 it is possible to notice in both bioreactors, the tissues of the *Scenedesmus* sp. in very good condition. Both in Figs. 9A and 9B, groups of four cells appear and also two cells in the process of dividing to multiply the colony. In the final stage of the culture carried out at pH 7.0, a lower cell concentration is observed than in the previous case, in both reactors, characterized by groups of four cells, as seen in Figs. 10A and 10B, although in the raceway bioreactor, a higher concentration of cellular biomass was achieved.

Regarding the cell state of the culture carried out at pH 7.5, however in appearance the image of Fig. 11B of the raceway reactor shows a higher cell concentration than the image of Fig. 11A of the tubular bioreactor, the culture of the raceway reactor shows deterioration in some organelles of its cells since the color is not homogeneous, and the cytoplasm is not attached to the cell wall and does not present the characteristic cilia of its species. For this test, a better final state of the culture was observed in the tubular reactor shown in Fig. 11A.

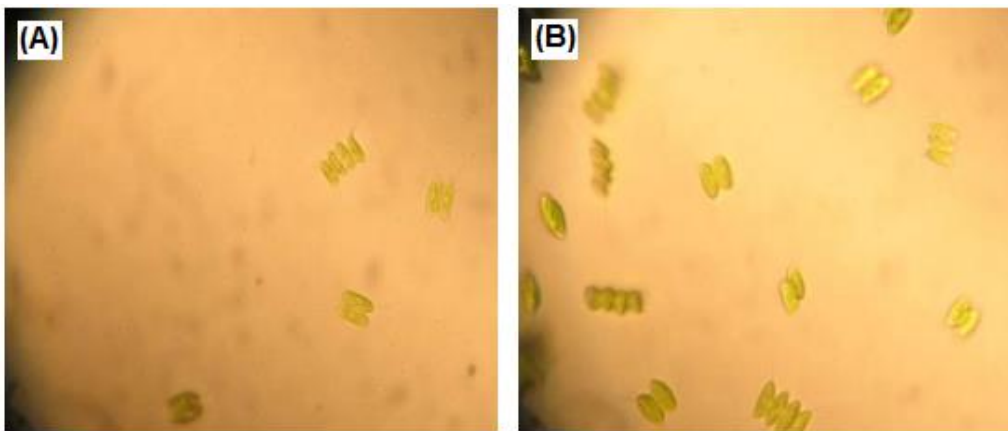


**Fig. 9** Final microscopy of the culture at pH = 6.5: (A) Tubular photobioreactor, (B) Raceway photobioreactor.

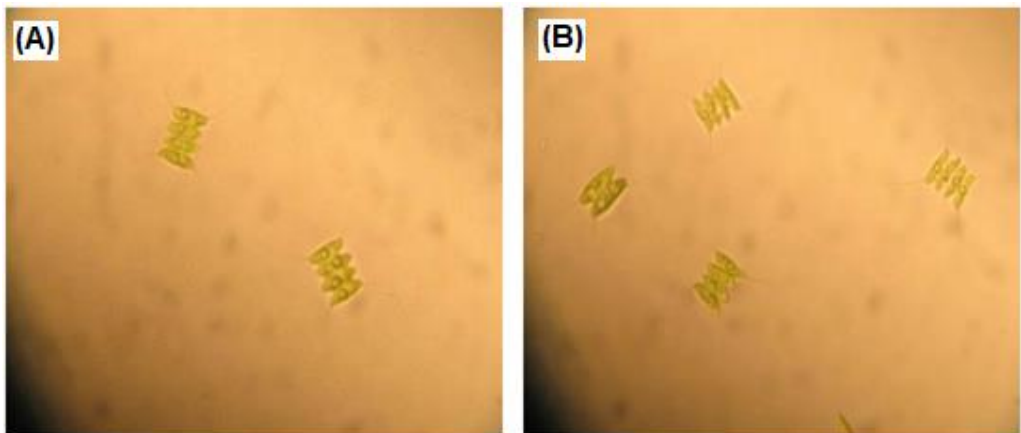


Fig. 10 Final microscopy of the culture at pH = 7.0: (A) Tubular photobioreactor, (B) Raceway photobioreactor.

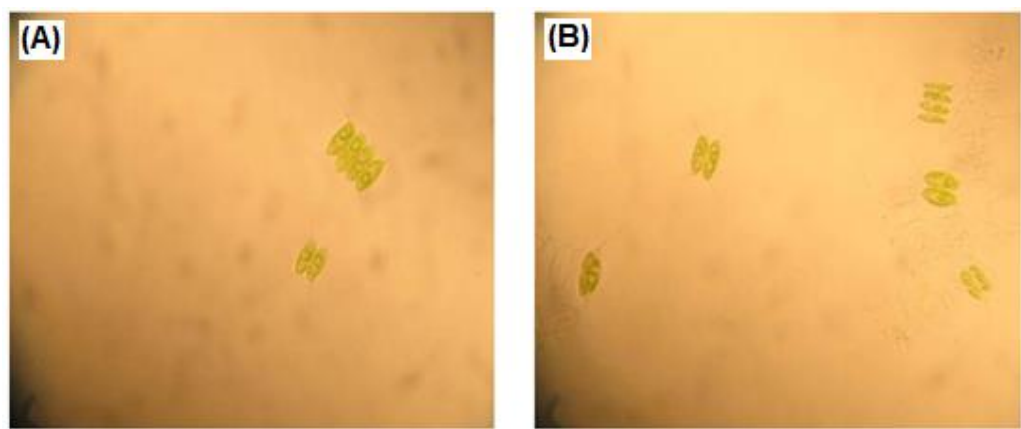


Fig. 11 Final microscopy of the culture at pH = 7.5: (A) Tubular photobioreactor, (B) Raceway photobioreactor.

#### 4. Conclusion

The most promising culture productivity conditions to grow the microalgae *Scenedesmus spinosus* in a pilot size photobioreactor, using Z-8 as culture medium, when comparing two different bioreactor design and a range of pH between 6.5 and 7.5 pH levels, turned out to be the lower pH level in the raceway modified bioreactor. At pH 6.5, the raceway bioreactor showed the best results in terms of final solid concentration and turbidity of the culture. The raceway photobioreactor performed better in terms of biomass productivity at the same pH value; however, the average irradiation on this bioreactor was significantly lower than the average irradiation levels of the tubular photobioreactor.

#### References

- [1] Kaberger, T. 2018. "Progress of Renewable Electricity Replacing Fossil Fuels." *Global Energy Interconnection* 1 (1): 48-52. <https://doi.org/10.14171/j.2096-5117.gei.2018.01.006>.
- [2] Bramstoft, R., Pizarro-Alonso, A., Jensen, I. G., Ravn, H., and Münster, M. 2020. "Modelling of Renewable Gas and Renewable Liquid Fuels in Future Integrated Energy Systems." *Applied Energy* 268: 114869. <https://doi.org/10.1016/j.apenergy.2020.114869>.
- [3] Bwapwa, J. K., Anandraj, A., and Trois, C. 2017. "Possibilities for Conversion of Microalgae Oil into Aviation Fuel: A Review." *Renewable and Sustainable Energy Reviews* 80: 1345-54. <https://doi.org/10.1016/j.rser.2017.05.224>.
- [4] Song, Ch., Liu, Q., Qi, Y., Chen, G., Song, Y., Kansha, Y., and Kitamura, Y. 2019. "Absorption-Microalgae Hybrid CO<sub>2</sub> Capture and Biotransformation Strategy—A Review." *International Journal of Greenhouse Gas Control* 88: 109-17. <https://doi.org/10.1016/j.ijggc.2019.06.002>.
- [5] Choi, Y., Patel, A. K., Hong, M. E., Chang, W. S., and Sim, S. J. 2019. "Microalgae Bioenergy with Carbon Capture and Storage (BECCS): An Emerging Sustainable Bioprocess for Reduced CO<sub>2</sub> Emission and Biofuel Production." *Bioresource Technology Reports* 7: 100270. <https://doi.org/10.1016/j.biteb.2019.100270>.

[6] Yang, Q., Li, H., Wang, D., Zhang, X., Guo, X., Pu, S., Guo, R., and Chen, J. 2020. "Utilization of Chemical Wastewater for CO<sub>2</sub> Emission Reduction: Purified Terephthalic Acid (PTA) Wastewater-Mediated Culture of Microalgae for CO<sub>2</sub> Bio-capture." *Applied Energy* 276: 115502. <https://doi.org/10.1016/j.apenergy.2020.115502>.

[7] Baicha, Z., Salar-García, M. J., Ortiz-Martínez, V. M., Hernández-Fernández, F. J., de los Ríos, A. P., Labjar, N., Lotfi, E., and Elmahi, M. 2016. "A Critical Review on Microalgae as an Alternative Source for Bioenergy Production: A Promising Low Cost Substrate for Microbial Fuel Cells." *Fuel Processing Technology* 154: 104-16. <https://doi.org/10.1016/j.fuproc.2016.08.017>.

[8] Dawes, C. J. 1986. "Botánica Marina." Limusa. México D.F., México.

[9] Arashiro, L. T., Boto-Ordóñez, M., Van Hulle, S. W. H., Ferrer, I., and A. Garfi, A. 2020. "D.P.L. Rousseau, Natural Pigments from Microalgae Grown in Industrial Wastewater." *Bioresource Technology* 303: 122894. <https://doi.org/10.1016/j.biortech.122894>.

[10] Pagels, F., Salvaterra, D., Amaro, H. M., and Guedes, A. C. 2020. "Fundamentals and Advances in Energy, Food, Feed, Fertilizer, and Bioactive Compounds." *Handbook of Microalgae-Based Processes and Products, Pigments from Microalgae* 18: 465-92.

[11] Morais, K. C. C., Conceição, D., Vargas, J. V. C., Mitchell, D. A., Mariano, A. B., Ordonez, J. C., Galli-Terasawa, L. V., and Kava, V. M. 2021. "Enhanced Microalgae Biomass and Lipid Output for Increased Biodiesel Productivity." *Renewable Energy* 163: 138-45. <https://doi.org/10.1016/j.renene.2020.08.082>.

[12] Talaghat, M. R., Mokhtari, Sh., and Saadat, M. 2020. "Modeling and Optimization of Biodiesel Production from Microalgae in a Batch Reactor." *Fuel* 280: 118578. <https://doi.org/10.1016/j.fuel.2020.118578>.

[13] De Jesus, S. S., Ferreira, G. F., Moreira, L. S., and Filho, R. M. 2020. "Biodiesel Production from Microalgae by Direct Transesterification Using Green Solvents." *Renewable Energy* 160: 1283-94. <https://doi.org/10.1016/j.renene.2020.07.056>.

[14] Aziz, Md. M. A., Kassim, K. A., Shokravi, Z., Jakarni, F. M., Liu, H. Y., Zaini, N., Tan, L. S., Saiful Islam, A. B. M., and Shokravi, H. 2020. "Two-Stage Cultivation Strategy for Simultaneous Increases in Growth Rate and Lipid Content of Microalgae: A Review." *Renewable and Sustainable Energy Reviews* 119: 109621. <https://doi.org/10.1016/j.rser.2019.109621>.

[15] Maxwell, J. R., Douglas, A. G., Eglington, G., and McCormick, A. 1968. "The Botryococcens-Hydrocarbons of Novel Structure from the Alga *Botryococcus Braunii*." *Kützing Phytochemistry* 7 (12): 2157-71. [https://doi.org/10.1016/S0031-9422\(00\)85672-1](https://doi.org/10.1016/S0031-9422(00)85672-1).

[16] Brown, A. C., Knights, B. A., and Conway, E. 1969. "Hydrocarbon Content and Its Relationship to Physiological State in the Green Alga *Botryococcus braunii*." *Phytochemistry* 8 (3): 543-7. [https://doi.org/10.1016/S0031-9422\(00\)85397-2](https://doi.org/10.1016/S0031-9422(00)85397-2).

[17] Fierro, S. 2004. "Utilización de microalgas inmovilizadas para la remoción de nutrientes de efluentes de cultivos acuícolas." Tesis, Maestría en Ciencias. Centro de Investigación Científica y de Educación Superior de Ensenada. Ensenada, México.

[18] Pandey, A., Gupta, A., Sunny, A., Kumar, S., and Srivastava, S. 2020. "Multi-objective Optimization of Media Components for Improved Algae Biomass, Fatty Acid and Starch Biosynthesis from *Scenedesmus* sp. ASK22 Using Desirability Function Approach." *Renewable Energy* 150: 476-86. <https://doi.org/10.1016/j.renene.2019.12.095>.

[19] Rocha, D. N., Martins, M. A., Soares, J., Gomes, M., Vieira Vaz, M., de O. Leite, M., Covell, L., and Mendes, L. B. B. 2019. "Combination of Trace Elements and Salt Stress in Different Cultivation Modes Improves the Lipid Productivity of *Scenedesmus* spp." *Bioresource Technology* 289: 121644. <https://doi.org/10.1016/j.biortech.2019.121644>.

[20] Keerthana, S., Sekar, S., Kumar, S. D., Santhanam, P., Divya, M., N. Krishnaveni, N., and Kim, M. K. 2020. "*Scenedesmus Pecensis* Cultivation in Rice Mill Effluent Using Commercial Scale Nutrient Sources." *Bioresource Technology Reports* 9: 100379. <https://doi.org/10.1016/j.biteb.2019.100379>.

[21] Barboza-Rodríguez, R., Rodríguez-Jasso, R. M., Rosero-Chasoy, G., Rosales Aguado, M. L., and Ruiz, H. A. 2024. "Photobioreactor Configurations in Cultivating Microalgae Biomass for Biorefinery." *Bioresource Technology* 394: 130208.

[22] Otalora, P., Skogestad, S., Guzmán, J. L., and Berenguel, M. 2024. "Modeling, Control and Online Optimization of Microalgae-Based Biomass Production in Raceway Reactors." *IFAC* 58 (14): 235-40.